

Zeeman-driven Lifshitz transition: A scenario for the Fermi-surface reconstruction in YbRh₂Si₂

Andreas Hackl¹ and Matthias Vojta²

¹*Department of Physics, California Institute of Technology, Pasadena, CA 91125, USA*

²*Institut für Theoretische Physik, Technische Universität Dresden, 01062 Dresden, Germany*

(Dated: February 16, 2022)

The heavy-fermion metal YbRh₂Si₂ displays a field-driven quantum phase transition where signatures of a Fermi-surface reconstruction have been identified, often interpreted as breakdown of the Kondo effect. We argue that instead many properties of the material can be consistently described assuming a Zeeman-driven Lifshitz transition of narrow heavy-fermion bands. Using a suitable quasiparticle model, we find a smeared jump in the Hall constant and lines of maxima in susceptibility and specific heat, very similar to experimental data. An intermediate non-Fermi liquid regime emerges due to the small effective Fermi energy near the transition. Further experiments to discriminate the different scenarios are proposed.

Quantum criticality in heavy-fermion metals constitutes an exciting and active research area [1, 2]. Among the various compounds investigated, CeCu_{6-x}Au_x and YbRh₂Si₂ stand out as possible candidates for the realization of a Kondo-breakdown quantum phase transition (QPT). Both display a transition from a non-magnetic to an antiferromagnetic (AF) metallic phase, with critical behavior which appears inconsistent with the predictions of the Landau-Ginzburg-Wilson (LGW) theory of three-dimensional (3d) AF criticality. This has prompted speculations about a novel class of QPT where the Kondo effect, responsible for the formation of heavy quasiparticles (QP), itself becomes critical, implying a reconstruction of the entire Fermi surface across the transition [3–5].

YbRh₂Si₂ [6], where the QPT is tuned by an applied magnetic field [7], is particularly interesting, because signatures of a Fermi-surface reconstruction have been identified in the Hall effect [8, 9]. Those measurements allowed to trace a line $T_{\text{Hall}}(B)$ in the temperature–field phase diagram where the crossover between two Fermi-surface configurations is supposed to occur, with the line terminating at the QPT at B_c and the crossover width $\Delta B(T)$ being approximately linear in temperature [9]. In addition, distinct changes in thermodynamic quantities have been employed to map out other crossover lines: magnetic susceptibility (χ), magnetization, and magnetostriction data result in a $T^*(B)$ line which roughly matches the $T_{\text{Hall}}(B)$ line [10, 11], while maxima in the specific heat coefficient, $\gamma = C/T$, lead to a lower $T_{\text{max}}(B)$ line, also terminating at the QPT at B_c [12]. Low- T Fermi-liquid behavior, identified by a T^2 behavior of the resistivity, sets in at an even lower $T_{\text{FL}}(B)$.

While the crossovers near the T^* and T_{Hall} lines are frequently assumed to be signatures of Kondo-breakdown quantum criticality, there are features which are not easily consistent with this hypothesis: (i) Under both isoelectronic doping and pressure, the magnetic phase boundary was found to move, while the T^* line moved very little [13, 14]. Assuming that (chemical) pressure

tunes the competition between Kondo screening and non-local interactions, the behavior of the T^* line is rather unexpected. (ii) Signatures of the T^* crossovers are never observed in zero field. (iii) In a T range between 0.1 and 1.5 K, $T^* = g^* \mu_B B$ [15] within error bars, with $g^* \approx 4.7$ for B applied in the a-b plane. In the same T range, $T_{\text{max}} = g_{\text{max}} \mu_B B$ with $g_{\text{max}} \approx 1.7$. This points towards Zeeman physics as a key player. (iv) In a quantum critical scenario, the T -linear width of the Hall crossover [9] suggests $\nu z = 1$, where ν and z are the correlation length and dynamical critical exponents. This is at odds with $\nu z \approx 0.7$ inferred from measurements of the Grüneisen parameters Γ_p [16] and Γ_H [17]. (v) Even at $B = B_c$, distinct low-temperature crossovers are seen in $C(T)$ [7, 12], $\Gamma_{p,H}(T)$ [16, 17], and the thermopower [18]. Thus, quantum criticality is at best restricted to very small T . Finally, we note that no theoretical modeling of the behavior near T_{Hall} , T^* is available to date.

In this Letter, we propose an alternative explanation for the intriguing crossovers in YbRh₂Si₂. Our scenario is that of a Fermi-surface reconstruction of a narrow heavy-fermion band (or piece thereof) via one or more Lifshitz transitions driven by Zeeman splitting [19, 20]. We shall show that this scenario naturally explains many elevated-temperature features, such as maxima in χ and γ at T^* , $T_{\text{max}} \propto B$ and a Hall crossover with a T -linear width. Importantly, these properties do *not* emerge in a quantum critical regime, but rather in a “high-temperature” regime above a tiny intrinsic energy scale (the depth of the assumed Fermi pockets). This regime is characterized by apparent non-Fermi liquid behavior, similar to the experimental data. Our scenario leads to a variety of predictions, to be tested in future experiments.

Band structure and Lifshitz transition. We shall assume that most of the physics of YbRh₂Si₂ at temperatures and fields below the Kondo scale, $T \ll T_0 \approx 20$ K and $B \ll B_0 \approx 10$ T, can be described in terms of heavy-fermion QP, implying that Kondo screening is effective near the T^* line [20].

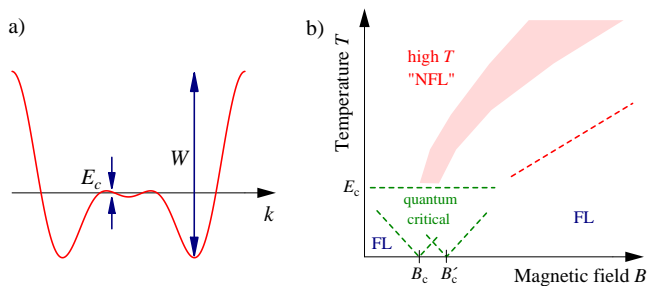


FIG. 1: a) Assumed band structure (schematic) of the heavy-fermion QP, with shallow Fermi pockets which induce a large zero-field DOS and lead to one (or more) field-induced Lifshitz transitions at small fields B_c , with $g\mu_B B_c \sim E_c$. b) Temperature-field phase diagram (schematic), with a quantum critical regime associated with the Lifshitz transitions at B_c, B'_c ; this regime is restricted to temperatures $T \ll E_c$ due to the small effective bandwidth E_c . The elevated-temperature regime, $T \gg E_c$, is characterized by apparent non-Fermi liquid behavior, with distinct crossovers occurring in the shaded region of the phase diagram, where the thermodynamics is that of a Zeeman-tuned Schottky anomaly.

Consider a band structure with an overall bandwidth W and a narrow piece of band at the Fermi level, the latter with a tiny effective bandwidth $E_c \ll W$ and a correspondingly small velocity (Fig. 1a). As a result, the zero-field density of states (DOS) displays a pronounced peak at the Fermi level, originating from Fermi pockets with an effective Fermi energy $\lesssim E_c$. Then, a tiny Zeeman field $g\mu_B B \sim E_c$, where g denotes the QP g factor, will split the bands such that the Fermi pockets disappear via zero-temperature Lifshitz transitions. At low temperatures, $T \ll E_c$, a standard quantum critical regime [23] near a critical field B_c marks the crossover between two Fermi-liquid regimes at small and large fields, the crossover being associated with a Fermi-surface reconstruction. (For a band structure as in Fig. 1a, there will be *two* separate Lifshitz transitions for the two spin species. Provided that the two critical fields are close, only measurements at ultralow temperatures, $T \ll g\mu_B |B_c - B'_c|$, will resolve two transitions.)

Most importantly, the Lifshitz-transition signatures in the T - B plane extend to temperatures much larger than E_c , because, as the DOS peak is split, the thermodynamics can be understood in terms of a Zeeman-tuned Schottky anomaly. As we shall demonstrate, quantities like $\chi(T)$ and $\gamma(T)$ generically display maxima at temperatures which follow $T \propto B$ for $T \gg E_c$. Moreover, interesting violations of Fermi-liquid behavior as function of T are found for temperatures above the scale B_c . Transport properties are similarly sensitive to the Lifshitz transitions and associated crossovers, and we will discuss the Hall effect below.

The results of this theoretical scenario match salient properties of YbRh_2Si_2 , assuming that $E_c \sim 50$ mK, $B_c \sim 50$ mT (for B in the a-b plane), while $W \sim 10$ – 20 K

is of order of the Kondo scale [15, 22].

Thermodynamics. For weakly interacting QP, thermodynamic quantities are entirely determined by the QP DOS $\rho(E)$. As elucidated above, the low-temperature and high-temperature regimes, characterized by $T \ll E_c$ and $E_c \ll T \ll W$ need to be distinguished. (The regime of $T \gtrsim W$ shall not be of interest here, as QP physics is not applicable for $T \gtrsim T_K$.)

For low T near a Zeeman-driven Lifshitz transition at B_c , analytical results can be easily derived [23]. Outside the critical regime, i.e., for $T \ll g\mu_B |B - B_c|$, the behavior is Fermi-liquid like, and the magnetic Grüneisen parameter (or magnetocaloric effect) is a constant reflecting the difference between the DOS of the two spin species, $\Gamma_H = -(dM/dT)/C_B \propto \rho_\uparrow - \rho_\downarrow$. In contrast, in the quantum critical regime, $g\mu_B |B - B_c| \ll T \ll E_c$, the free energy follows $F \propto T^{1+d/2}$ for a band-edge singularity in d space dimensions. The critical piece of the specific heat is then $C_{\text{cr}} \propto T^{d/2}$, similar to that of the magnetization, $M_{\text{cr}} \propto T^{d/2}$. Taking into account the Fermi-liquid background contribution, this results in $\Gamma_H \propto T^{d/2-2}$, with the sign depending on the type of Lifshitz transition: If pockets disappear (appear) with increasing field, then $\Gamma_H > 0$ ($\Gamma_H < 0$). If the quantum critical regimes of two nearby Lifshitz transitions overlap (Fig. 1b), then the critical contributions to thermodynamic quantities simply add, without further qualitative changes. For YbRh_2Si_2 these results apply to $T \ll 50$ mK.

More relevant is the high-temperature regime, which – upon tuning B – will be dominated by the competition between the two scales B and T , resulting in crossovers as function of $g\mu_B B/T$. Concrete results in this regime depend on the DOS on all energies up to $\max(g\mu_B B, T)$, but some effects can be illustrated in the narrow-band limit, i.e., in a toy model of a Zeeman-split local fermionic level at $\pm h$ with $h = g\mu_B B/2$. For $T \gg h$, $\chi \propto 1/T$. For fixed h , $\chi(T)$ has a maximum at $T^*/h = 0.65$ whereas $\gamma(T)$ has a maximum at $T_{\text{max}}/h = 0.31$ [24].

A full set of numerical results is presented in Fig. 2, for free fermions with the sample DOS shown in Fig. 2a. This DOS has two step discontinuities (e.g. from band edges in 2d), leading to two nearby Lifshitz transitions at h_c, h'_c . While Fermi-liquid laws are obeyed at asymptotically low T at all fields away from the Lifshitz transitions, they are generically violated at elevated T . In particular, near h_c , $\gamma(T)$ shows a weak apparent divergence for $T > 0.1$, with a pronounced upturn for $T < 0.1$ and saturation only for $T < 0.005$, while $\chi(T)$ follows an approximate power law $T^{-0.6}$ down to $T = 0.05$ before it saturates. A field cuts off the apparent low-temperature singularities, leading to maxima in $\gamma(T)$ and $\chi(T)$ for $h > h_c, h'_c$. These maxima follow $T^*, T_{\text{max}} \propto h$ with $T^*/T_{\text{max}} \approx 2.1$ over an intermediate range of fields (physics of a Schottky anomaly), but the non-zero background DOS induces a curvature which becomes significant at large fields. The magnetocaloric effect is posi-

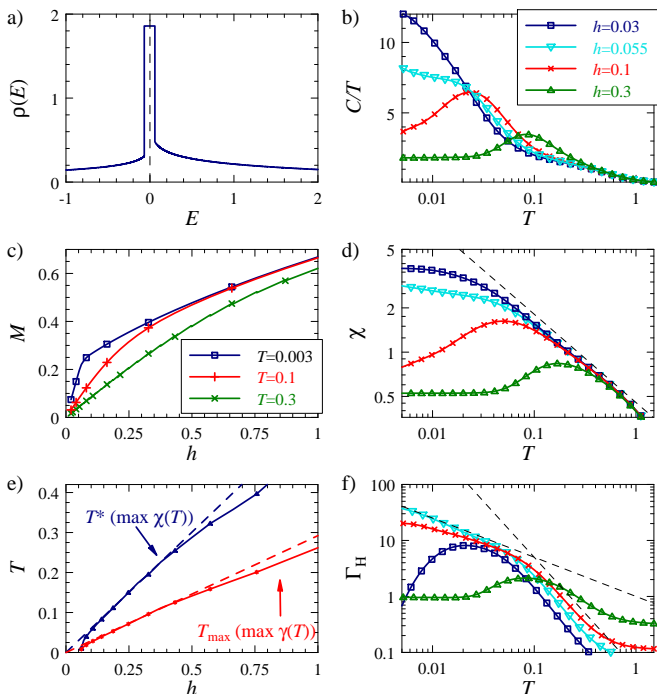


FIG. 2: Thermodynamic properties near a Zeeman-driven Lifshitz transition. a) Input DOS $\rho(E)$ with bandwidth $W = 4$ and a low-energy peak of width $E_c = 0.12$. Step discontinuities are crossed at fields $h_c = 0.055$ and $h'_c = 0.08$, $h = g\mu_B B/2$. b) Specific heat coefficient $\gamma(T)$ for different applied fields. c) Magnetization $M(h)$, showing a pronounced kink at a temperature-dependent field. d) Magnetic susceptibility $\chi(T)$; the dashed line is a power law $\chi \propto T^{-0.6}$. e) Location of maxima in $\chi(T)$ and $\gamma(T)$ in the T - h phase diagram; the dashed lines are linear fits through the origin. f) Magnetocaloric effect $\Gamma_H(T)$; the dashed lines show power laws $\Gamma_H \propto T^{-0.7}$ and T^{-2} .

tive; near h_c it displays a crossover between two apparent power laws, $\Gamma_H \propto T^{-0.7}$ for $T < 0.05$ and $\Gamma_H \propto T^{-2}$ for $0.1 < T < 0.7$ – the latter strong divergence is rooted in the apparent divergence of $\chi(T)$, together with the weak T dependence of γ . (The critical $\Gamma_H \propto 1/T$ is seen at h_c, h'_c only for $T < 0.005$.) It should be emphasized that none of the power laws above $T = 0.01$ is of asymptotic character; they rather represent crossover behavior arising from the interplay of peak and background DOS. Consequently, the exponents are non-universal. We note that the precise *shape* of the DOS peak is unimportant for $T \gtrsim E_c$, in particular, 3d Lifshitz transitions yield qualitatively similar results.

Transport and Hall effect. In contrast to thermodynamics, transport properties depend on the actual band structure. In the absence of detailed experimental or ab-initio information [22], we focus on the shape and width of the crossover in the Hall constant R_H at a generic Zeeman-driven Lifshitz transition. Being interested in $T, B \ll T_K$, we shall employ a Boltzmann approach with momentum-independent QP scattering rate

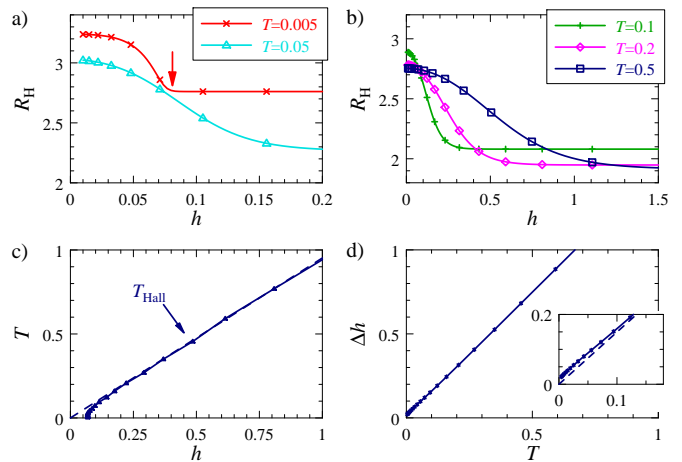


FIG. 3: Hall coefficient of a square-lattice tight-binding model with hopping 0.05 and filling 1.7. The Zeeman-driven Lifshitz transition is at $h_c = 0.08$. a, b) $R_H(h)$ for different temperatures. The sharp crossover at low T arises from the Lifshitz transition (arrow). c) Location of the Hall crossover in the T - h phase diagram, defined by the maximum location of $|dR_H/dh|$. d) Full width at half maximum of $|dR_H/dh|$.

[25]. In this approximation, the critical piece follows $R_{H,cr} \propto (h_c - h)^{d/2}$ at $T = 0$ (while non-critical Zeeman-induced changes in R_H are linear in h).

Sample results for the Hall constant are shown in Fig. 3 for a square-lattice tight-binding model. R_H approaches constant values in the limits of small and large fields, with a pronounced crossover in between. For $T \rightarrow 0$, this “smeared step” can be understood as follows: On the high-field side, there is a kink at the Lifshitz transition (Fig. 3a), while the behavior on the low-field side arises from deviations from parabolic dispersion. The location and width of the crossover peak in dR_H/dh at fixed T allow to extract a crossover line $T_{Hall}(h)$ and width $\Delta h(T)$, plotted in Figs. 3c and d. (Note that the peak position in dR_H/dh for $T \rightarrow 0$ does not coincide with the precise location of the Lifshitz transition.) The behavior of $T_{Hall}(h)$ is similar to that of T^* and T_{max} , with a large-field slope of $T_{Hall}/h \approx 0.98$ [26]. The crossover width varies linearly with T with a small offset of $\Delta h(T \rightarrow 0) \approx h_c/4$. This saturation signals that the $T = 0$ behavior of $R_H(h)$ is continuous. Importantly, the T -linear width is a result of thermal smearing, not of collective effects. We have verified that the qualitative results are generic for Lifshitz transitions in both 2d and 3d (up to a non-critical background in R_H arising from other bands). In application to YbRh_2Si_2 , our results imply that the crossover width arising from a Lifshitz transition can well “look” T -linear down to 30 mT.

Discussion. So far, collective instabilities of the heavy QP are not included in the description. They can be expected to be important at low T : Plugging the large-field g factor of 3.6 into the QP calculation, the field-

induced energy and temperature scales are too small by a factor of 3–4, as seen in the slopes of T^* and T_{\max} . A plausible explanation is a large enhancement of the low-field g factor due to incipient ferromagnetism. Indeed, the QP Zeeman splitting can be strongly enhanced by ferromagnetic correlations [21], known to be present in YbRh_2Si_2 [27].

Which experiments can reliably distinguish between the scenarios of (i) a Kondo-breakdown transition and (ii) a Zeeman-driven Lifshitz transition as source of the Fermi-surface reconstruction? The principal distinction is that in (i) the low-field phase in the absence of magnetism is expected to be a true non-Fermi liquid, i.e., a metallic spin liquid, most likely of the fractionalized Fermi-liquid type [5]. In contrast, in (ii) all phases have Fermi-liquid character in the low-temperature limit, with $\gamma \rightarrow \text{const}$ and the Wiedemann-Franz law being satisfied. Experiments on Ir-doped or Ge-doped YbRh_2Si_2 [13, 14], where magnetism is suppressed down to very low T and B , can access this region of the phase diagram. The practical problem is that probing the true low- T behavior requires temperatures significantly below 50 mK. Existing data do not cover this regime in a sufficient manner.

A further distinction is in the response of the phase boundary and crossover lines to changes in system parameters, such as doping and pressure. Scenario (i) implies that the T^* line arises from the competition between Kondo screening and inter-moment interactions, and thus should be sensitive to changes in the hybridization strength induced by pressure. In contrast, in scenario (ii) the phase boundary will be more robust and only react to strong changes in hybridization matrix elements or in the electron concentration. Existing data, where (chemical) pressure has little influence on the T^* line [13, 14], appear more consistent with (ii). Thus, we propose to study YbRh_2Si_2 using dopants with different valence. Here, an influence on the phase boundary can be expected for sizeable doping levels.

Our scenario yields a connection between incipient ferromagnetism and the slopes of the T^* and T_{\max} lines. If certain dopants enhance (reduce) the ferromagnetic tendencies, then those slopes should increase (decrease).

Finally, we touch upon the role of AF. This is an instability independent of the Lifshitz transition, but the two may influence each other depending on Fermi-surface details. Fluctuations of AF order will influence both thermodynamics and transport at low T near the AF transition, e.g., they will modify the upturn in $\gamma(T)$. Inside the AF phase, it is conceivable that strong ordering will modify the band structure such that the shallow Fermi pockets are removed from the Fermi level. Hence, we predict that the low- T part of the T^* line will be smeared in sufficiently Co-doped YbRh_2Si_2 .

Summary. We have shown that key features of the field-driven QPT in YbRh_2Si_2 can be consistently explained in the framework of Zeeman-driven Lifshitz tran-

sition, with Kondo screening remaining intact. Zeeman splitting of shallow Fermi pockets causes anomalies in both thermodynamic and transport properties, including apparent non-Fermi liquid behavior. Most remarkable is a smeared jump in the Hall constant upon variation of the field which signals a Fermi surface reconstruction, with a crossover width proportional to T over a wide range of temperatures. While it is clear that collective effects are relevant at very low temperatures, our results suggest that a large portion of the YbRh_2Si_2 phase diagram can be understood in terms of QP Lifshitz physics.

We enjoyed extensive exchange with M. Brando, P. Gegenwart, and O. Stockert, who suggested the relevance of Zeeman physics in YbRh_2Si_2 . We further thank S. Friedemann, A. Rosch, F. Steglich, and P. Wölfle for discussions. This research was supported by DFG FOR 960.

-
- [1] P. Gegenwart *et al.*, Nature Phys. **4**, 186 (2008).
 - [2] H. v. Löhneysen *et al.*, Rev. Mod. Phys. **79**, 1015 (2007).
 - [3] P. Coleman, C. Pépin, Q. Si, and R. Ramazashvili, J. Phys: Condens. Matt. **13**, R723, (2001).
 - [4] Q. Si *et al.*, Nature (London) **413**, 804 (2001).
 - [5] T. Senthil *et al.*, Phys. Rev. Lett. **69**, 216403 (2003).
 - [6] O. Trovarelli *et al.*, Phys. Rev. Lett. **85**, 626 (2000).
 - [7] P. Gegenwart *et al.*, Phys. Rev. Lett. **89**, 056402 (2002).
 - [8] S. Paschen *et al.*, Nature **432**, 881 (2004).
 - [9] S. Friedemann *et al.*, PNAS **107**, 14547 (2010).
 - [10] P. Gegenwart *et al.*, J. Phys. Soc. Jpn. **75** Suppl., 155 (2006).
 - [11] P. Gegenwart *et al.*, Science **315**, 969 (2007).
 - [12] N. Oeschler *et al.*, Physica B **403**, 1254 (2008).
 - [13] S. Friedemann *et al.*, Nature Phys. **5**, 465 (2009).
 - [14] J. Custers *et al.*, Phys. Rev. Lett. **104**, 186402 (2010).
 - [15] We employ units where $k_B = 1$.
 - [16] R. KÜchler *et al.*, Phys. Rev. Lett. **91**, 066405 (2003).
 - [17] Y. Tokiwa *et al.*, Phys. Rev. Lett. **102**, 066401 (2009).
 - [18] S. Hartmann *et al.*, Phys. Rev. Lett. **104**, 096401 (2010).
 - [19] A link between Zeeman physics and T^* was proposed before in S. V. Kusminskiy *et al.*, Phys. Rev. B **77**, 094419 (2008), but the relevant crossovers were not studied.
 - [20] A QP description has been successfully employed to model the ESR spectra observed in YbRh_2Si_2 [21].
 - [21] P. Wölfle and E. Abrahams, Phys. Rev. B **80**, 235112 (2009).
 - [22] Present-day ab-initio techniques cannot give reliable information on the band structure on scales below 1 meV.
 - [23] S. Sachdev, *Quantum Phase Transitions*, Cambridge University Press, Cambridge (1999).
 - [24] For a Zeeman-split local level, the maximum position in $\chi(T)$ is found from solving $xn_F''(x) + n_F'(x) = 0$ with $x = h/T$ and n_F the Fermi function, resulting in $x = 1.54$. Similarly, the maximum in $\gamma(T)$ follows from $xn_F''(x) + 3n_F'(x) = 0$ with the solution $x = 3.24$.
 - [25] While the scattering rate from impurities will be affected by a Lifshitz transition, those changes will cancel in R_H .
 - [26] Different crossover criteria [8, 9] may lead to T_{Hall} values which differ by a factor of two for fixed B , due to the asymmetric R_H crossover [S. Friedemann, priv. comm.].
 - [27] P. Gegenwart *et al.*, Phys. Rev. Lett. **94**, 076402 (2005).